

Cite this: *Nanoscale Adv.*, 2020, 2, 3788

# Development of biological metal–organic frameworks designed for biomedical applications: from bio-sensing/bio-imaging to disease treatment

Huai-Song Wang,\* Yi-Hui Wang and Ya Ding \*

Metal–organic frameworks (MOFs) are built using various organic ligands and metal ions (or clusters). With properties of high porosity, tunable chemical composition, and potential for post-synthetic modification, they have been applied in biomedicine, especially in bio-sensing, bio-imaging, and drug delivery. Since organic ligands and metal centers (ions or clusters) in the structure of MOFs can directly influence the property, function, and performance of MOFs, strict screening of organic ligands and metal centers is necessary. Especially, to improve the application of MOFs in the field of biomedicine, biocompatible organic ligands with low toxicity are desirable. In recent years, biological metal–organic frameworks (bio-MOFs) with ideal biocompatibility and diverse functionality have attracted wide attention. Endogenous biomolecules, including nucleobases, amino acids, peptides, proteins, porphyrins and saccharides, are employed as frameworks for MOF construction. These biological ligands coordinate with diverse metal centers in different ways, leading to the structural diversity of bio-MOFs. In this review, we summarize the organic ligand selectivity in constructing different types of bio-MOFs and their influence in biomedical applications with attractive new functions.

Received 6th July 2020  
Accepted 30th July 2020DOI: 10.1039/d0na00557f  
rsc.li/nanoscale-advances

## 1. Introduction

Metal–organic frameworks (MOFs) are composed of organic ligands and metal ions (or clusters). With properties of large surface area, high porosity, tunable chemical composition, and potential for post-synthetic modification,<sup>1–5</sup> different types of MOFs have been developed and applied in many important fields, such as gas storage/separation, catalysis, molecular

sensing, and biomedicine.<sup>6–8</sup> Especially, in the field of biomedicine, MOFs show many advantages, including high porosity, diverse structures, adjustable surface function and biodegradability.<sup>9–12</sup> The particle composition, size and morphology of MOFs can be easily adjusted to optimize their functions. The diverse internal high porosity of MOFs provides spaces for encapsulating a large number of drugs, biological molecules, and emissive dyes, as well as nanomaterials with biological functions. So far, there have been many reports about MOFs for bio-sensing, bio-imaging, and disease treatment.<sup>13,14</sup>

Key Laboratory of Drug Quality Control and Pharmacovigilance (Ministry of Education), China Pharmaceutical University, Nanjing, 210009, China. E-mail: wanghuaisong@cpu.edu.cn; dingya@cpu.edu.cn



Huai-Song Wang received his PhD in analytical chemistry in 2011 from Nankai University. After completing postdoctoral research at Nanjing University in 2014, he joined the faculty of the College of Pharmaceutical Analysis of China Pharmaceutical University. He is now an associate professor. His current research interest is primarily in the area of designing functional metal–organic frameworks for

biosensing and bioimaging.

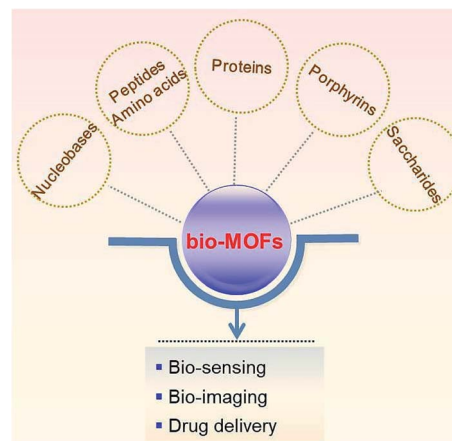


Yi-Hui Wang was born in Shanxi, China. She received her bachelor's degree in Traditional Chinese Medicine pharmacy from China Pharmaceutical University (2020). She is currently a master of Pharmaceutical analysis under the supervision of Prof. Huai-Song Wang. Her research interest focuses on biosensors for nucleic acids.



For bio-sensing or bio-imaging, the luminescence properties of MOFs can be bestowed by the introduction of either organic ligands or metal centers (ions or clusters) with intrinsic luminescence properties, or luminescent guest molecules or ions.<sup>15–17</sup> For drug delivery or disease treatment, several limitations of guest drugs can be well resolved after they are encapsulated in the pore structures or constructed in the frameworks of MOFs, including poor solubility, blood instability, and systemic toxicity due to the wide drug distribution in the whole body.

Since organic ligands directly influence the biomedical applications of MOFs, strict screening of organic ligands is necessary.<sup>18–20</sup> In order for MOFs to be better applied in the field of biomedicine, organic ligands of MOFs with good biocompatibility and low toxicity have been employed. So far, there have been some reviews about the application of nanoscale metal–organic-frameworks in the biomedical field.<sup>21</sup> This review focuses on metal–organic-framework based biological endogenous molecules, so their biocompatibility is self-evident. As for the biocompatibility of metal–organic frameworks, some binding modes are also widely involved, such as guest molecule loading, surface modification and directly as organic ligands to construct metal–organic frameworks.<sup>22,23</sup> This review mainly discusses metal–organic frameworks formed by biological endogenous molecules directly coordinated with metal ions as organic ligands, called bio-MOFs, which emphasize the composition as biocompatible materials. In recent years, bio-MOFs have attracted wide attention due to their ideal biocompatibility and diverse functionality. Bio-MOFs are prepared by using biological endogenous organic ligands, including nucleobases, amino acids, peptides, proteins, porphyrins and saccharides. These biological ligands have diverse coordination ways with metal centers, leading to the diverse structures and functions of bio-MOFs (Scheme 1). In the past three years, new preparation methods and applications of bio-MOFs have made great progress. Therefore, there is large space for summary and discussion of bio-MOFs. In this review, we will summarize



Scheme 1 Bio-MOFs prepared using biological organic ligands for biomedicine.

different types of bio-MOFs designed for biomedical applications, including bio-sensing, bio-imaging, and disease treatment. Furthermore, the future challenges and outlook of bio-MOFs are also discussed.

## 2. Designing bio-MOFs with bio-ligands

As a subclass of MOFs, bio-MOFs possess both the porous properties of MOFs and the physiological functions of biomolecular ligands. The structural diversity of bio-ligands (including nucleobases, amino acids, peptides, proteins, porphyrins and saccharides) can determine the biomedical performances of bio-MOFs. And, the presence of bio-ligands enhances the biocompatibility of bio-MOFs, which makes them more suitable to be used in the biomedical field. Herein, different bio-ligands for designing bio-MOFs will be introduced.

### 2.1 Nucleobase ligands

Nucleobases provide a large number of strong hydrogen bonding moieties, such as oxygen-containing and nitrogen-containing sites, and possess strong coordination ability with metal ions.<sup>24,25</sup> The rigid molecular structure of nucleobases can facilitate the formation of stable cavities in porous bio-MOFs. The formation of these bio-MOFs is generally achieved *via* deprotonation of nucleobases during the coordination with metal centers. Polycarboxylate ligands can be used as auxiliary ligands to prepare the diverse structures of bio-MOFs.<sup>26</sup>

Nucleobases are mainly divided into two types: purines and pyrimidines. Purines (adenine and guanine) are more suitable as biological ligands than pyrimidines (thymine and cytosine), because of their more coordination sites.<sup>27</sup> For example, adenine contains 5 different nitrogen atoms, an N<sub>6</sub> amino group and N<sub>1</sub>, N<sub>3</sub>, N<sub>7</sub> and N<sub>9</sub> imino-nitrogens,<sup>28</sup> which have strong coordination behavior with metal ions. Recently, a type of bio-MOF, SION-19, was synthesized based on the ligand of adenine (Ade), which enabled the cavity of SION-19 to contain



*Ya Ding is a full professor of Pharmaceutical Analysis at China Pharmaceutical University, China. She received her Ph.D. degree in Analytical Chemistry from Nanjing University (2007). She was a post-doctoral fellow from 2008–2012 in the Department of Biology, Nanjing University and a visiting scholar from 2013–2014 in the Department of Chemistry, at the University of Massachusetts-*

*Amherst. Her research interests focus on new materials and technologies for pharmaceutical analysis and disease treatment. She is the awardee of the Program for New Century Excellent Talents in University (2010) and Science Technology Achievement Award, Higher Institution (Natural Science Award, the first prize, 2011).*



the Watson–Crick surface: the basic unit of the hydrogen bond that formed the DNA double helix.<sup>29</sup> SION-19 was prepared by the reaction of  $\text{Zn}(\text{NO}_3)_2 \cdot 6\text{H}_2\text{O}$ , 1,3,6,8-tetrakis(*p*-benzoic acid) pyrene ( $\text{H}_4\text{TBAPy}$ ) and Ade (Table 1). In the structure of SION-19 (Fig. 1), the octahedral cage was composed of four Ade ligands and six  $\text{Zn}^{2+}$ . Ade was used as a tridentate ligand for bridging, while the deprotonated TBAPy formed a complex in monodentate coordination. Based on the coordination property above, the pores of SION-19 can be divided into acid pores and base pores. The size of acid pores is  $7.9 \text{ \AA} \times 4.9 \text{ \AA}$ , with free carboxylate groups of TBAPy; while the size of base pores is  $5.4 \text{ \AA} \times 6.9 \text{ \AA}$ , with an unobstructed Watson–Crick surface provided by Ade. For application, SION-19 can capture thymine (Thy) through hydrogen bonding, achieving A–T base pairing in the cavity of SION-19. Thus, SION-19 can simulate the role of DNA, which can be used as a nanoreactor. Furthermore, this new type of bio-MOF can be potentially used for the adsorption and separation of specific molecules, targeted drug delivery, and solid-phase catalytic reactions.

Another Ade based bio-MOF was reported for enhancing enzyme activity.<sup>30</sup> Methionine adenosyltransferase (MAT), a type of enzyme that can catalyze the reaction of methionine and ATP to generate *S*-adenosylmethionine, was encapsulated in a bio-MOF prepared by the coordination of Ade and  $\text{Zn}^{2+}$ . The formed enzyme/bio-MOF hybrid nanomaterial,  $\text{MAT@Zn}_2(\text{Ade})$ , can enhance the activity and stability of MAT. Furthermore, under extreme conditions (such as temperature changes, acidic

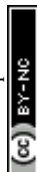
conditions, protease and organic solvent erosion), it can maintain long-term stability. At pH 3 and  $80^\circ\text{C}$ ,  $\text{MAT@Zn}_2(\text{Ade})$  still showed strong catalytic activity. This research indicated that bio-MOFs have a promising future to be used in the field of enzyme protection, enhancing the activity of enzymes.

Cytosine and guanine have also recently been used for preparing bio-MOFs. Sarma and co-workers reported that cytosine (or guanine) can coordinate with  $\text{Zn}^{2+}$  under deprotonated conditions, forming a type of metal gel with nanofiber morphology.<sup>31</sup> And, the coordination interaction between  $\text{Zn}^{2+}$  and a mixture of the two nucleobases can produce a hybrid flower like superstructure. The self-assembled bio-MOFs exhibited semiconducting characteristics for environmental purification by photocatalytic degradation of pollutant dyes (methylene blue, MB).

Other nucleobase based bio-MOFs, such as water-stable bio-MOF-11-Co (prepared by the coordination of  $\text{Co}^{2+}$  and Ade) also showed degradation ability toward guest molecules.<sup>32</sup> Bio-MOF-11-Co with submicron size exhibited rapid degradation behavior toward *para*-hydroxybenzoic acid (*p*-HBA) and sulfa-chloropyridazine (SCP), which are hazardous chemicals existing in wastewater. Additionally, nucleobase based bio-MOFs can be prepared with emissive properties, which can increase their application field. For example, bioMOF-Zn, coordinated by 4,4'-biphenyl-dicarboxylic acid (BPDC) and Ade, showed strong blue emission and can be observed by the naked eye.<sup>33</sup> BioMOF-Zn showed excellent loading capacity ( $1.72 \text{ g g}^{-1}$ ) and release

Table 1 Bio-MOFs prepared using bio-ligands for separation, catalysis and bio-sensing

| Bio-MOFs  | Bio-ligands                                       | Metal ions                          | Auxiliary ligands            | Targets                  | Limit of detection                     | Potential applications  | Ref. |
|---|---|-------------------------------------|------------------------------|--------------------------|--|---|------|
| SION-19   | Adenine   | $\text{Zn}^{2+}$                    | $\text{H}_4\text{TBAPy}$     | —                        | —                                      | Molecular adsorption and separation, solid-phase catalytic reaction | 29   |
| $\{\text{CaCu}_6[(S,S)\text{-serimox}]_3(\text{OH})_2(\text{H}_2\text{O})\} \cdot 39\text{H}_2\text{O}$ (-Ca) | Serimox = bis [( <i>S</i> -serine] oxalyl diamide | $\text{Ca}^{2+}$ , $\text{Cu}^{2+}$ | —                            | B-vitamin                | —                                      | Molecular recognition and extraction                                | 37   |
| $\text{MAT@Zn}_2(\text{adenine})$   | Adenine   | $\text{Zn}^{2+}$                    | —                            | MAT                      | —                                      | Enzyme protection   | 30   |
| —   | PLGA ( $\gamma$ -poly-L-glutamic acid)            | $\text{Zn}^{2+}$                    | HmIM                         | —                        | —                                      | Biomacromolecule protection   | 41   |
| $\text{Zn}(\text{CG})_n$  | Cytosine guanine                                  | $\text{Zn}^{2+}$                    | —                            | Methylene blue (MB)      | —                                      | Photocatalytic degradation  | 31   |
| Bio-MOF-11  | Adenine   | $\text{Co}^{2+}$                    | —                            | <i>p</i> -HBA, SCP       | —                                      | Catalytic degradation   | 32   |
| $\text{Zn}(\text{Glu})$   | L-Glutamic acid                                   | $\text{Zn}^{2+}$                    | —                            | Cyclic carbonate         | —                                      | Cycloaddition catalysis   | 35   |
| $\text{Cu}(\text{Trp})$   | L-Tryptophan                                      | $\text{Cu}^{2+}$                    | —                            | Cyclic carbonate         | —                                      | Cycloaddition catalysis   | 36   |
| Co-P-MOF  | Aspartic acid                                     | $\text{Co}^{2+}$                    | —                            | Asymmetric sulfuroxide   | —                                      | Cross-coupling reaction catalysis                                   | 42   |
| bisH-SF   | Ferritin  | $\text{Ni}^{2+}$                    | His <sub>2</sub>             | —                        | —                                      | Enzymatic catalysis   | 45   |
| MIP-202(Zr)   | L-Aspartic acid                                   | $\text{Zr}^{4+}$                    | —                            | —                        | $1.1 \times 10^{-2} \text{ S cm}^{-1}$ | Electrochemical detection   | 39   |
| $\text{MnO}_2$ NFs  | BSA   | $\text{Mn}^{2+}$                    | —                            | Glucose                  | $1 \times 10^{-6} \text{ M}$           | Glucose colorimetric detection                                      | 44   |
| $\text{Eu}^{3+}\text{-TTA@ bio-MOF-1}$  | Adenine   | $\text{Zn}^{2+}$                    | —                            | Organic amine            | —                                      | Fluorescent probe   | 57   |
| PCN-222   | TCPP  | $\text{Zr}^{4+}$                    | —                            | Phosphoprotein(a-casein) | $0.13 \text{ \mu g mL}^{-1}$           | Photoelectrochemical sensor   | 58   |
| $\{\text{CuTCPP}[\text{AlOH}]_2\}_n$  | TCPP  | $\text{Cu}^{2+}$                    | —                            | $\text{H}_2\text{S}$     | 16 nM                                  | Fluorescent probe   | 59   |
| R-Uio   | $\text{H}_2\text{DBP-Pt}$                         | $\text{Hf}^{4+}$                    | $\text{H}_2\text{QPDC-NH}_2$ | $\text{O}_2$             | 0.017 mm $\text{Hg}^{-1}$              | Phosphorescence/fluorescence dual-emissive probe                    | 60   |
| dye@ZnBTCA  | Adenine   | $\text{Zn}^{2+}$                    | —                            | Temperature              | 260 K                                  | Fluorescence ratio probe  | 61   |
| Eu@1  | $\text{H}_3\text{TAPB}$                           | $\text{Zn}^{2+}$ , $\text{Eu}^{3+}$ | —                            | $\text{Cu}^{2+}$         | 0.01 mM                                | Fluorescent probe   | 62   |



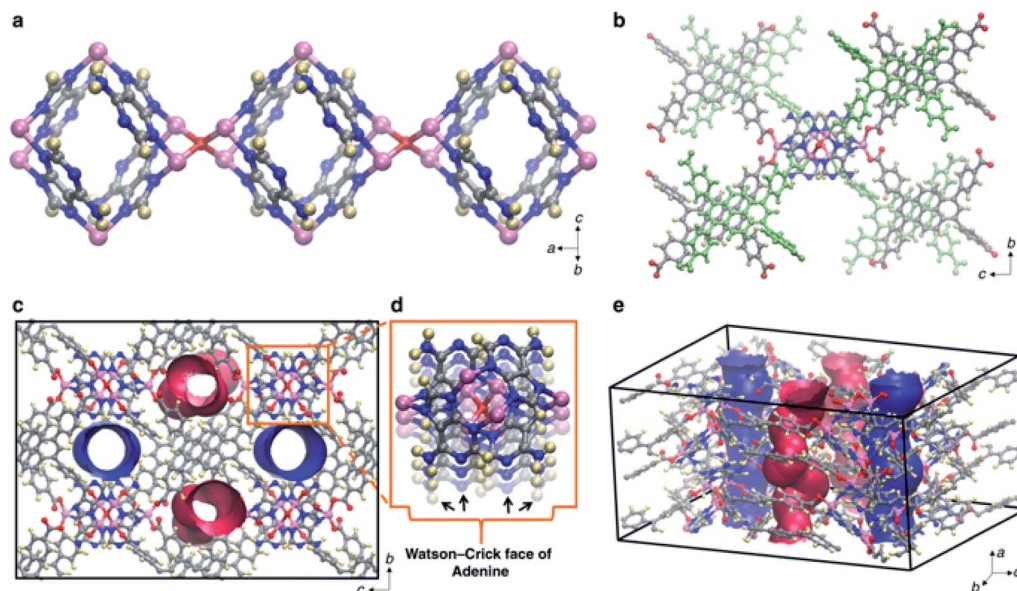


**Fig. 1** Structural simulation of SION-19. (a) and (b) Three-dimensional structures of SION-19 at different scales, where pink represents Zn atoms, red represents O atoms, blue represents N atoms, gray represents C atoms, and yellow represents H atoms. (c–e) The pore structure of SION-19. (d) Watson–Crick surface provided by Ade. Reproduced from ref. 29 with permission from Nature Publishing Group.

capacity (56% after two days) for diclofenac sodium, and can be further used for drug delivery.

## 2.2 Amino acid ligands

Amino acids, containing both carboxyl ( $-\text{COOH}$ ) and amino ( $-\text{NH}_2$ ) groups, are ideal ligands for preparing bio-MOFs. In proteins, the side chain of amino acids can affect the overall hydrophilic or hydrophobic character, which will influence subsequent protein formation and functions. Therefore, the amino groups, carboxyl groups and side chains of amino acids can provide multiple coordination ways, making them a type of promising organic ligand for bio-MOFs. However, research studies have shown that amino acid based bio-MOFs are hardly prepared with high porosity. This might be because of the closed groups of  $-\text{COOH}$  and  $-\text{NH}_2$  in the structures of amino acid molecules. Therefore, the modification of natural amino acids and using auxiliary ligands are needed to expand the porosity of multi-dimensional bio-MOFs.<sup>34</sup>

Recently, a type of water-stable amino acid based bio-MOF with 3D topology was reported by the coordination of *L*-glutamic acid as the bio-ligand and  $\text{Zn}^{2+}$  as the metal ion.<sup>35</sup> The prepared bio-MOF ( $\text{ZnGlu}$ ) with open metal sites was successfully used for the catalytic synthesis of cyclic carbonate from  $\text{CO}_2$ . Furthermore, another amino acid-based bio-MOF,  $\text{CuTrp}$  with catalytic properties, was prepared by the coordination of *L*-tryptophan (Trp) and  $\text{Cu}^{2+}$ .<sup>36</sup>  $\text{CuTrp}$  showed good catalytic activity and recyclability in the catalytic preparation of cyclic carbonates from epoxides and  $\text{CO}_2$ .

Amino acid based bio-MOFs have also been designed for selective guest molecule adsorption. For example, the bio-MOF derived from *L*-serine can be used as an adsorbent for B-vitamin molecular recognition and extraction;<sup>37</sup> a zinc glutamate bio-

MOF was synthesized and supported on cellulose fabrics for drug loading and controlled release.<sup>38</sup> Nitric oxide (NO) and 5-fluorouracil (5-FU) loaded in the bio-MOF were controlled released relying on the acid environment of pathological sites.

In the field of electrochemistry, amino acid based bio-MOFs have shown their advantages. A zirconium bio-MOF, MIP-202(Zr), composed of *L*-aspartic acid, showed a high and stable proton conductivity of  $0.011 \text{ s cm}^{-1}$  at 363 K and 95% relative humidity.<sup>39</sup> Fig. 2 shows the structure of MIP-202(Zr). The stability of MIP-202(Zr) was proved to be better than previously reported Zr-MOFs prepared using aromatic carboxylic acid linkers. Furthermore, MIP-202(Zr) not only exhibited excellent stability in water, but also had significant tolerance to both acidic and alkaline conditions. MIP-202(Zr) with the proton conduction ability can be potentially used as a promising candidate in electroanalytical chemistry for biological molecule detection.

## 2.3 Peptide ligands

Peptides, composed of amino acids, are important options for regulating physiological functions.<sup>40</sup> Due to different stereo structures and conformations of amino acids, peptides with inherent chirality have specific targeting ability in biological systems. The peptide structure can be adjusted by changing the type and order of amino acids. The diversity of peptides enables them to contain multiple coordination sites, which can be employed to synthesize multi-dimensional bio-MOFs.

PLGA ( $\gamma$ -poly-*L*-glutamic acid) is a type of anionic peptide with rich carboxyl groups, and has been employed as a surface modification moiety for preparing biomacromolecules through electrostatic interaction. Thereby, the properties of PLGA greatly promote the formation of peptide based bio-MOFs. Recently,



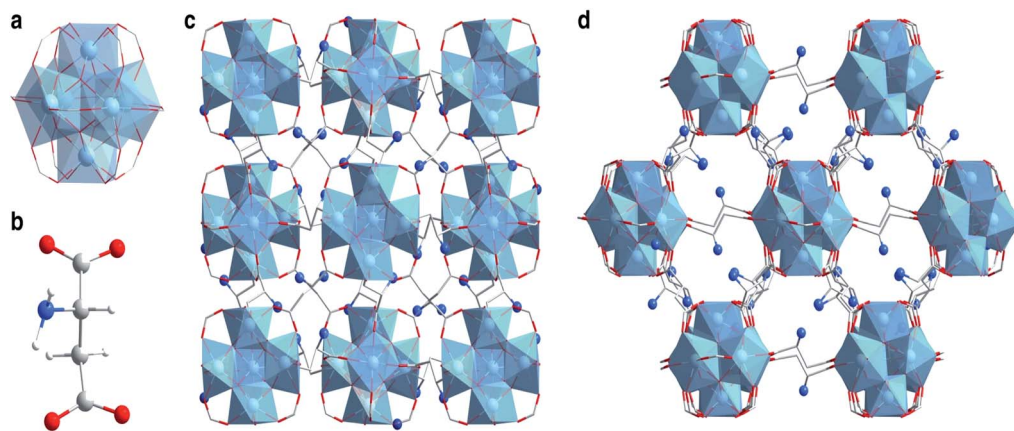


Fig. 2 Crystal structures of MIP-202(Zr). (a) The 12-connected  $Zr_6(\mu_3-O)_4(\mu_3-OH)_4(COO^-)_{12}$  cluster SBU. (b) The aspartic acid linker. (c and d) The structure of MIP-202(Zr) viewed along the  $a$ -axis (c) and the (101) plane (d). Zr atoms or polyhedra, oxygen, carbon, nitrogen, and hydrogen atoms are respectively shown with colors of light blue, red, gray, dark blue, and white. Reproduced from ref. 39 with permission from Nature Publishing Group.

Ouyang and co-workers reported a type of PLGA biohybrid ZIF-8 for protecting and enhancing the properties of bio-macromolecules or proteins.<sup>41</sup> In the bio-composite, the excess PLGA chains can competitively interact with metal ions through carboxyl groups, leading to morphological evolution and defective structure formation (Fig. 3). This gentle strategy can evaluate the protection effect of MOF nanostructures on the activity of biological macromolecules. Compared with widely studied 3D MOF composites, the prepared MOF biohybrid showed a significant advantage in the protection of host proteins and retained their functionalities.

Cobalt containing compounds generally possess catalytic properties for chemical reactions. Recently, a type of chiral bio-MOF (Co-P-MOF), prepared using cobalt and aspartic acid-based peptides, was successfully used for asymmetric sulfoxidative cross-coupling.<sup>42</sup> It can be used to catalyze the

asymmetric synthesis of chiral sulfoxides from cross coupling reaction of aryl halides, phenylboronic acid and poly sulfynylpiperazine (as novel S=O transfer agent). Therefore, peptides, with chiral characteristics, have special molecular recognition ability. The formed bio-MOFs may have potential applications in asymmetric catalysis, as well as in enantiomeric separation.

#### 2.4 Protein ligands

Because of the flexibility and complexity of the protein structure, the coordination between metal ions and the protein interface is difficult to control.<sup>43</sup> However, due to the versatility and diversity of protein molecules, the development of protein-based bio-MOFs still has a good prospect. For example,  $Mn^{2+}$  can spontaneously oxidize to  $MnO_2$  crystals in alkaline solution, and BSA can be used as the skeleton and stabilizer.<sup>44</sup> The

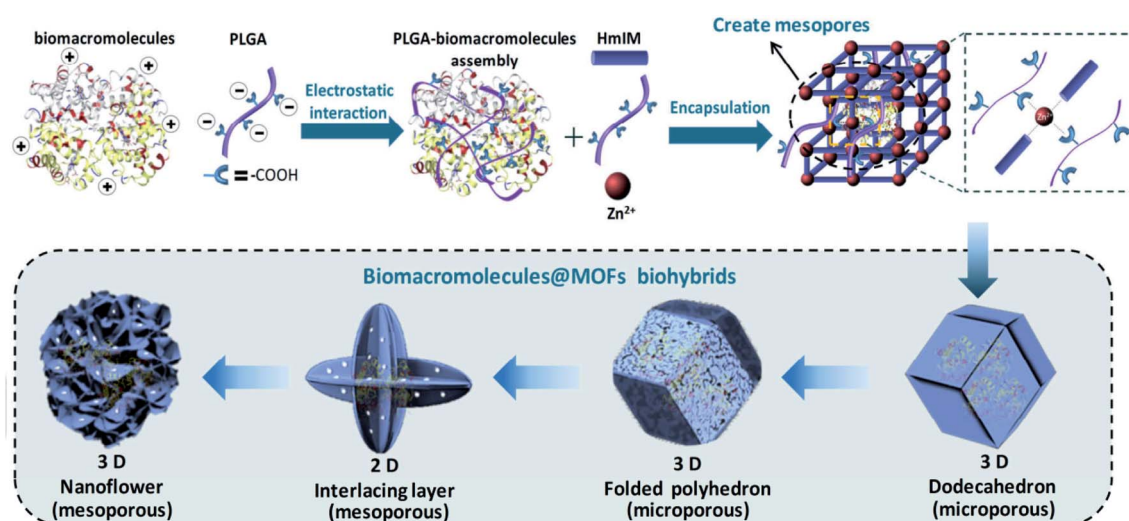


Fig. 3 Illustration of the deformable MOF by using a PLGA modulator. Reproduced from ref. 41 with permission of WILEY-VCH Verlag GmbH & Co. KGaA, Weinheim.



morphologically controlled MnO<sub>2</sub> nanosheet was obtained by changing reaction conditions. It was found that the material has tandem enzymatic characteristics (namely glucose oxidase-like activity and peroxidase-like activity). Then the colorimetric assay of glucose based on one-pot enzyme-free catalysis was proposed. This method has a high sensitivity, low detection limit and short detection time.

Ferritin is widely found in living organisms and usually consists of 24 subunits assembled into hollow protein shells with octahedral symmetry. Ferritin has been studied as a nano-platform for preparing various nanomaterials or as a carrier for tumor imaging and treatment. Recently, a strategy for the manufacture of binary MOFs was proposed.<sup>45</sup> Considering the symmetry of octahedral ferritin, four His<sub>2</sub> (His-His) patterns, which replaced Thr157 located on the outer surface of the C-4 symmetry axis, were mixed with the outer surface of ferritin nanocages near each C-4 channel to produce protein joints (bisH-SF). Then, the addition of nickel ions to the bisH-SF solution triggered the self-assembly of ferritin nanocages into a porous 3D-crystal MOF with a designed protein lattice, where two adjacent ferritin molecules (along C-4 symmetry axis) were bridged by four binuclear or quad-nuclear nickel clusters (depending on Ni<sup>2+</sup> concentration) (Fig. 4). This work provided a simple method for control of binary protein-metal crystal frames, and the resulting MOF exhibited intrinsic ferric oxidase activity and peroxidase-like catalytic activity.

## 2.5 Porphyrin ligands

Porphyrins are a class of macromolecular compounds containing  $\alpha$ -carbon atoms of four pyrrole subunits connected with a methine bridge (=CH).<sup>46</sup> Porphyrins have good biocompatibility, specific targeting for tumor tissues and no obvious toxic and side effects on normal cells, so they are widely used in the biomedical field. In addition, porphyrins have potential value in biomimetic catalysis. So they are suitable as biological ligands for preparing bio-MOFs. Tetra (4-carboxyphenyl) porphyrin (H<sub>4</sub>TCPP) is one of the most commonly used porphyrin ligands for the construction of porphyrin metal organic frameworks. TCPP and Zr<sub>6</sub> clusters can form a series of MOFs named PCN.<sup>47</sup>

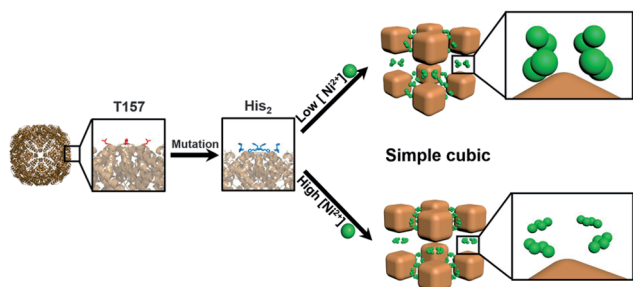


Fig. 4 Self-assembly of ferritin nanocages into 3D crystals with a cubic lattice through Ni<sup>2+</sup> clusters upon the replacement of T157 (red) by His<sub>2</sub> (blue) near the C-4 channels for Ni<sup>2+</sup> (green). Reproduced from ref. 45 with permission of WILEY-VCH Verlag GmbH & Co. KGaA, Weinheim.

PCN-224 is composed of Zr<sup>4+</sup> and TCPP ligands, which are coordinated by covalent bonds.<sup>48</sup> Zr<sup>4+</sup> is used for the combination with bridged ligands to prepare an ultra-stable Zr-MOF. The photosensitizer TCPP can be employed to construct PCN-224 (Fig. 5). Due to the easy diffusion of oxygen through the porous MOF structure, the resulting porphyrin-type MOF structure had high light-to-oxygen generation. The porphyrin MOF-based nanoprobe can effectively inhibit the self-assembly of monomer A $\beta$  into a  $\beta$ -sheet structure under the excitation of near infrared light. In addition, light-excited PCN-224 also significantly reduced A $\beta$ -induced cytotoxicity under near infrared radiation. The photo-oxidation treatment triggered by this porphyrin MOF-based nanoprobe will have good applications in neurodegenerative diseases such as Alzheimer's disease. Platinum nanoparticles are evenly fixed on PCN-224, with stability and catalase-like activity.<sup>49</sup> This strategy used oxygen produced by hydrogen peroxide to improve the hypoxic environment of tumors. Thereby, this can generate singlet oxygen causing greater damage to tumors by PDT. Zr clusters are multivalently coordinated with the HA's carboxylic acid.<sup>50</sup> Thus, HA can stably cover the surface of the MOF. HA can allow drug carriers to selectively aggregate in CD44 overexpressed cancer cells and release enzyme-responsive drugs in the environment of cancer cells. This HA-PCN system combined chemotherapy and photodynamic therapy to improve the therapeutic effect on tumors.

## 2.6 Saccharide ligands

Saccharides have been applied as building blocks for self-assembled structures, which become effective host molecules. Among them, cyclodextrins (CDs) with special structures are important host molecules.<sup>51</sup> Cyclodextrin (CD) is the general name for a series of cyclic oligosaccharides produced by the action of amylase.  $\alpha$ ,  $\beta$ , and  $\gamma$ -cyclodextrins are cyclic oligomers composed of 6, 7, and 8 D (+)-glucopyranose. These molecules with a cylindrical shape are wide at the top, narrow at the bottom, and open at both ends. And it is relatively hydrophobic inside the cavity, while all hydroxyl groups are outside the molecule.

A type of nanoporous cyclodextrin MOF (CD-MOF) crystal suitable for dry powder inhalation (DPI) and aerodynamic deposition was prepared and used for drug delivery.<sup>52</sup> The CD-MOF, composed of  $\gamma$ -cyclodextrin ( $\gamma$ -CD) and potassium ions, was used as the DPI carrier for pulmonary delivery of budesonide (BUD). Cholesterol (CHO) was applied to modify the CD-

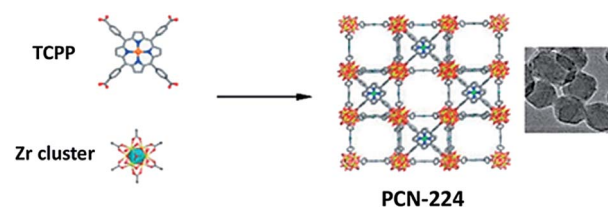


Fig. 5 Schematic illustration of the synthesis of PCN-224 nanoparticles. Reproduced from ref. 48 with permission of American Chemical Society.



MOF powder to improve the fluidity and aerodynamic performance of the particles. The drug effectively entered the lungs *via* the prepared CHO-CD-MOF, which can be used as a promising DPI carrier for drug delivery with a small dose.

The  $\gamma$ -CD based CD-MOF, synthesized from the coordination of  $\gamma$ -CD and KOH by the vapor diffusion approach, can also be used as a carrier of methotrexate (MTX).<sup>53</sup> The inclusion formation of MTX with  $\gamma$ -CD increased the dissolution rate of drugs and slightly reduced the permeability of drugs through the lipophilic membrane. The authors predict that the drug delivery system can be used for oral drug absorption with minimal adverse effects.

## 2.7 Other biomolecule based ligands

Besides nucleobases, amino acids, peptides, proteins, porphyrins, and saccharides, some other biologically active small molecules can also be used as bio-ligands to coordinate with metals to form novel bio-MOFs. Acid biomolecules, such as formic acid, oxalic acid, and fumaric acid, containing carboxylic acid groups have been used as organic ligands. Recently, some therapeutic molecules with coordination groups have also been used to prepare bio-MOFs for biomedical applications. Curcumin (CCM), a polyphenolic pigment found in turmeric roots, is a natural compound with  $C_{2v}$  bilateral symmetry. Its uniqueness lies in its three ionizable protons, two of which come from phenol groups and the other from enol groups. CCM has different metal binding sites and exhibits a variety of possible coordination modes (Fig. 6). This feature increases its potential structural diversity when it is used as a multidentate linker to react with metal ions. CCM is also helpful in treating chronic diseases including cancer, inflammatory diseases and neurological diseases. By coordinating with  $Zn^{2+}$ , CCM can be used as a bio-ligand to prepare a bio-MOF,  $[Zn(\text{curcumin})]_n$ , called sc-CCMOF-1.<sup>54</sup> As a system of a releasable active agent, the bio-MOF was specially applied in CCM delivery.

$Mg^{2+}$  deficiency may influence the pathways of osteoarthritis (OA) pathology. Preparing  $Mg^{2+}$  based bio-MOFs for  $Mg^{2+}$  delivery to treat OA is an ideal choice. Tang and co-workers designed a type of  $Mg^{2+}$  based bio-MOF,  $Mg/\text{HCOOH-MOF}$  by using formic acid as the ligand, to achieve long-term release of  $Mg^{2+}$  for the treatment of OA.<sup>55</sup> As a type of nano-drug, the  $Mg/\text{HCOOH-MOF}$  is stable in biological systems and can release  $Mg^{2+}$  continuously. Long-term application of the  $Mg/\text{HCOOH-MOF}$  can promote the proliferation of MG63 cells, significantly up-regulate the expression of osteogenic genes, and contribute to bone formation and resorption. In addition, it can obviously reduce the expression of inflammatory genes and has anti-inflammatory effects on subchondral bone. Therefore, the  $Mg/\text{HCOOH-MOF}$  is considered to be a potential nano-drug for the treatment of OA.

5-Borobenzene 1,3-dicarboxylic acid (BBDC) with boric acid groups has been used as a ligand to react with glucose, increasing the biocompatibility of MOFs. Recently, Yin and co-workers reported a type of BBDC based bio-MOF for imaging-guided chemotherapy.<sup>56</sup> The bio-MOF was prepared by the coordination of BBDC as the ligand and  $Gd^{3+}$  as the metal center. Glucose was coated on the surface of the bio-MOF *via* the specific reversible condensation of diol and borate, thus improving its biocompatibility. The interaction between glucose and glucose transporters ensured successful tumor targeting. In addition, the glucose layer acted as a pH responsive moiety to prevent drug leakage. The anti-cancer drug DOX can be loaded in the MOF, and used as an intelligent nano-system for MR image-guided tumor targeted therapy (Fig. 7). At present, the imaging-guided drug release by using bio-MOFs has made some progress, but it is still in the primary stage. The systematic study of the stability, biocompatibility and toxicity of bio-MOFs in a biological environment still needs deep exploration.

The bio-MOFs mentioned above are listed in the following tables. The typical characteristics of the bio-MOFs discussed in

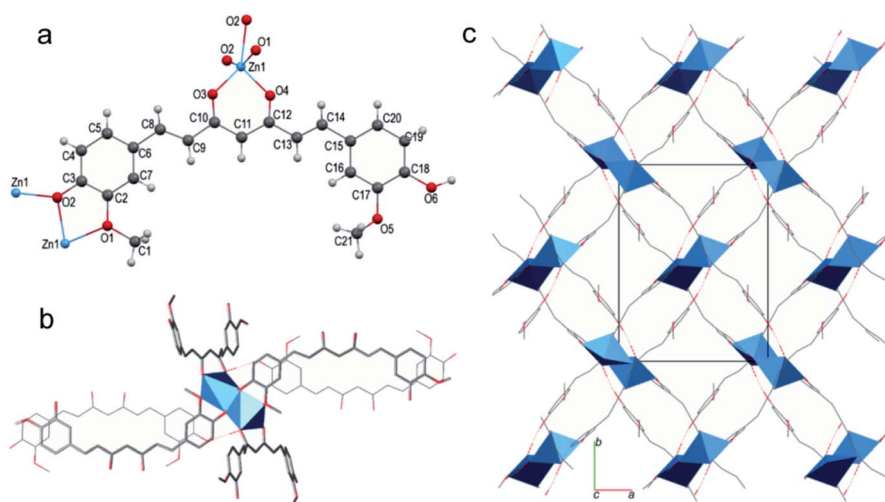


Fig. 6 The structure of sc-CCMOF-1: (a) the coordination mode; (b) the  $Zn_2O_8$  SBU structure and (c) the 2D framework. Reproduced from ref. 54 with permission of American Chemical Society.



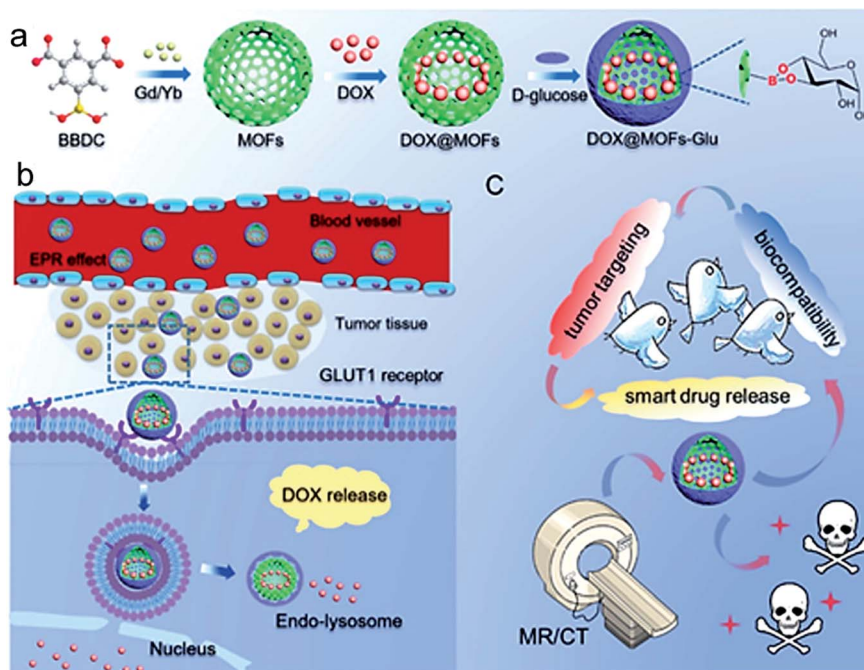


Fig. 7 DOX@MOFs-glucose for image-guided tumor targeted therapy. (a) Preparation method for DOX@MOFs-glucose. (b) Drug release mechanism. (c) Multifunction of the nanocarrier for imaging-guided drug release. Reproduced from ref. 56 with permission of American Chemical Society.

Table 2 Bio-MOFs prepared using bio-ligands for bio-imaging and drug delivery

| Bio-MOFs  | Bio-ligands                                | Metal ions       | Auxiliary ligands                          | Imaging methods  | Therapeutic methods                           | Target diseases  | Ref. |
|---|--|------------------|--|------------------|---|--|------|
| SION-19   | Adenine                                    | Zn <sup>2+</sup> | H <sub>4</sub> TBAPy                       | —                | Chemotherapy                                  | Targeted drug delivery   | 29   |
| Bio-MOF-Zn  | Adenine                                    | Zn <sup>2+</sup> | 4,4'-Biphthalic acid (BPDC)                | —                | Diclofenac sodium release                     | Drug release OA/RA therapy   | 33   |
| Zn(Glu)   | L-Glutamic acid                            | Zn <sup>2+</sup> | —  | —                | Chemotherapy (NO, 5-Fu)                       | Drug delivery  | 38   |
| PCN-224   | TCPP                                       | Zr <sup>4+</sup> | —  | —                | Photo-oxidation treatment                     | Neurodegenerative disease therapy  | 48   |
| PCN-224 Pt  | TCPP                                       | Zr <sup>4+</sup> | Pt   | —                | PDT   | Tumor therapy  | 49   |
| HA-PCN  | TCPP                                       | Zr <sup>4+</sup> | HA   | —                | Chemotherapy, PDT                             | Tumor therapy  | 50   |
| CHO-CD-MOF  | γ-CD                                       | K <sup>+</sup>   | CHO  | —                | Budesonide (BUD) release                      | Budesonide (BUD) DPI carrier   | 52   |
| γ-CD-MOF  | γ-CD                                       | K <sup>+</sup>   | —  | —                | Chemotherapy (MTX), immune system suppressant | Tumor therapy  | 53   |
| sc-CCMOF-1  | Curcumin (CCM)                             | Zn <sup>2+</sup> | —  | —                | CCM release                                   | Drug delivery, cancer, inflammatory disease and neurological disease therapy | 54   |
| Mg/HCOOH-MOF                                      | HCOOH                                      | Mg <sup>2+</sup> | —  | —                | Mg <sup>2+</sup> release                      | OA therapy   | 55   |
| Gd-MOFs   | 5-Borobenzene 1,3-dicarboxylic acid (BBDC) | Gd <sup>3+</sup> | —  | MRI/CT           | Chemotherapy (DOX)                            | Drug release, bio-imaging  | 56   |
| ZrMOF   | DNA  | Zr <sup>4+</sup> | —  | Targeted imaging | PDT   | Tumor therapy, bio-imaging   | 63   |
| isMOFs  | Cytosine-phosphate-guanosine (CpG)         | Zr <sup>4+</sup> | —  | —                | DNA therapy                                   | Drug release   | 64   |
| TTA-UC MOF  | TCPP                                       | Zr <sup>4+</sup> | DCDPA                                      | Optical imaging  | —   | Bio-imaging  | 65   |
| Fe-MIL-53-NH <sub>2</sub> -FA-5-FAM/5-FU          | FA   | Fe <sup>3+</sup> | NH <sub>2</sub> -H <sub>2</sub> BDC, 5-FAM | FI/MRI           | Chemotherapy (5-fu)                           | Drug delivery, bio-imaging   | 66   |
| <sup>89</sup> Zr-Uio-66/Py-PGA-PEG-F <sub>3</sub> | F <sub>3</sub> peptide                     | Zr <sup>4+</sup> | BDC, BA,                                   | PET              | —   | Bio-imaging  | 67   |





this review for bio-sensing are listed in Table 1, including sensing targets, limits of detection, and the potential applications of the bio-MOF based sensors. And, bio-MOFs for bio-imaging and disease treatment are listed in Table 2. The imaging methods, therapeutic methods and target diseases of the bio-MOFs are summarized.

### 3. Conclusion and outlook

MOFs applied in the field of biomedicine not only need to achieve the required functions for bio-sensing, bio-imaging, and drug delivery, but also need good biocompatibility. The use of biological endogenous molecules as organic ligands to form bio-MOFs can potentially meet these two requirements. Biological ligands have multiple coordination sites, self-assembly capabilities, chirality, and hydrophobic and hydrophilic tendencies. At the same time, many bio-ligands have chiral conformations, so they can be used to construct bio-MOFs with chiral recognition, separation and catalytic behaviors.

Although bio-MOFs have made great progress in preparation and biomedical applications, there are still some biological application challenges that need to be addressed. First, the interaction between metal ions and biological ligands needs to be systematically studied, which can provide a reasonable principle system for the design of bio-MOFs. Second, it is necessary to develop simple, controllable and cost-effective methods for preparation, and investigate the influence of solvents, temperature, pH, *etc.* on material synthesis, to ensure suitable size, uniform shape and processability of bio-MOFs. Third, the thermal and chemical stability and water stability of bio-MOFs still need to be strengthened, otherwise, it will limit their development in biological applications. Furthermore, a detailed understanding of the interaction between bio-MOFs and cells is essential, which will help further imaging and treatment systems. Bio-MOFs should have a suitable circulation time *in vivo*, and then actively or passively target tumor cells to be specifically internalized. After exerting their efficacy, they should degrade without affecting normal cells. This is related to the toxicity of bio-MOFs. Bio-MOFs with good biocompatibility and low toxicity will bring great progress to biomedical applications. Finally, the mechanism of bio-MOFs overcoming barriers *in vivo* and a series of subsequent processes (such as biological absorption, distribution, transformation, metabolism and excretion) require in-depth study. It is believed that bio-MOFs will become a type of materials with excellent biological structure and function, which can be applied in the biomedical field in the future.

### Conflicts of interest

The authors declare no competing financial interest.

### Acknowledgements

This work was supported by the National Natural Science Foundation of China (21705165 and 31870946), the Funding of

Double First-rate discipline construction (CPU2018GF07, China), the Fundamental Research Funds for the Central Universities, and a Project Funded by the Priority Academic Program Development of Jiangsu Higher Education Institutions.

### References

- 1 H.-C. Zhou, J. R. Long and O. M. Yaghi, *Chem. Rev.*, 2012, **112**, 673–674.
- 2 S. Kitagawa, R. Kitaura and S. Noro, *Angew. Chem., Int. Ed.*, 2004, **43**, 2334–2375.
- 3 O. M. Yaghi, G. Li and H. Li, *Nature*, 1995, **378**, 703–706.
- 4 D. Britt, D. Tranchemontagne and O. M. Yaghi, *Proc. Natl. Acad. Sci. U. S. A.*, 2008, **105**, 11623–11627.
- 5 H. Furukawa, N. Ko, Y. B. Go, N. Aratani, S. B. Choi, E. Choi, A. O. Yazaydin, R. Q. Snurr, M. O’Keeffe, J. Kim and O. M. Yaghi, *Science*, 2010, **329**, 424–428.
- 6 A. Schneemann, V. Bon, I. Schwedler, I. Senkovska, S. Kaskel and R. A. Fischer, *Chem. Soc. Rev.*, 2014, **43**, 6062–6096.
- 7 M. L. Foo, R. Matsuda and S. Kitagawa, *Chem. Mater.*, 2014, **26**, 310–322.
- 8 A. Betard and R. A. Fischer, *Chem. Rev.*, 2012, **112**, 1055–1083.
- 9 M. Paul and P. Dastidar, *Chem.–Eur. J.*, 2016, **22**, 988–998.
- 10 C. He, D. Liu and W. Lin, *Chem. Rev.*, 2015, **115**, 11079–11108.
- 11 F.-Y. Yi, D. Chen, M.-K. Wu, L. Han and H.-L. Jiang, *Chempluschem*, 2016, **81**, 675–690.
- 12 D. Liu, K. Lu, C. Poon and W. Lin, *Inorg. Chem.*, 2014, **53**, 1916–1924.
- 13 P. Horcajada, R. Gref, T. Baati, P. K. Allan, G. Maurin, P. Couvreur, G. Férey, R. E. Morris and C. Serre, *Chem. Rev.*, 2012, **112**, 1232–1268.
- 14 M. Gimenez-Marques, T. Hidalgo, C. Serre and P. Horcajada, *Coord. Chem. Rev.*, 2016, **307**, 342–360.
- 15 D. Zou, J. Zhang, Y. Cui and G. Qian, *Dalton Trans.*, 2019, **48**, 6669–6675.
- 16 H.-S. Wang, *Coord. Chem. Rev.*, 2017, **349**, 139–155.
- 17 Y. Liu, X.-Y. Xie, C. Cheng, Z.-S. Shao and H.-S. Wang, *J. Mater. Chem. C*, 2019, **7**, 10743–10763.
- 18 S. Beg, M. Rahman, A. Jain, S. Saini, P. Midoux, C. Pichon, F. J. Ahmad and S. Akhter, *Drug Discovery Today*, 2017, **22**, 625–637.
- 19 R. J. Kuppler, D. J. Timmons, Q.-R. Fang, J.-R. Li, T. A. Makal, M. D. Young, D. Yuan, D. Zhao, W. Zhuang and H.-C. Zhou, *Coord. Chem. Rev.*, 2009, **253**, 3042–3066.
- 20 Z. Ma and B. Moulton, *Coord. Chem. Rev.*, 2011, **255**, 1623–1641.
- 21 S. Li, L. Tan and X. Meng, *Adv. Funct. Mater.*, 2020, **30**, 1908924.
- 22 K. Lu, T. Aung, N. Guo, R. Weichselbaum and W. Lin, *Adv. Mater.*, 2018, **30**, e1707634.
- 23 S. Wang, C. M. McGuirk, A. d’Aquino, J. A. Mason and C. A. Mirkin, *Adv. Mater.*, 2018, **30**, e1800202.
- 24 G. Beobide, O. Castillo, A. Luque and S. Perez-Yanez, *Crystengcomm*, 2015, **17**, 3051–3059.



- 25 Z.-J. Lin, J. Lu, M. Hong and R. Cao, *Chem. Soc. Rev.*, 2014, **43**, 5867–5895.
- 26 Pratibha and S. Verma, *Cryst. Growth Des.*, 2015, **15**, 510–516.
- 27 F. H. Allen, *Acta Crystallogr., Sect. B: Struct. Sci.*, 2002, **58**, 380–388.
- 28 G. Beobide, O. Castillo, J. Cepeda, A. Luque, S. Perez-Yanez, P. Roman and J. Thomas-Gipson, *Coord. Chem. Rev.*, 2013, **257**, 2716–2736.
- 29 S. L. Anderson, P. G. Boyd, A. Gladysiak, T. N. Nguyen, R. G. Palgrave, D. Kubicki, L. Emsley, D. Bradshaw, M. J. Rosseinsky, B. Smit and K. C. Stylianou, *Nat. Commun.*, 2019, **10**, 1612.
- 30 J. He, S. Sun, M. Lu, Q. Yuan, Y. Liu and H. Liang, *Chem. Commun.*, 2019, **55**, 6293–6296.
- 31 B. Sharma, A. Mahata, S. Mandani, N. Thakur, B. Pathak and T. K. Sarma, *New J. Chem.*, 2018, **42**, 17983–17990.
- 32 M. R. Azhar, P. Vijay, M. O. Tade, H. Sun and S. Wang, *Chemosphere*, 2018, **196**, 105–114.
- 33 G. N. Lucena, R. C. Alves, M. P. Abuçafy, L. A. Chiavacci, I. C. da Silva, F. R. Pavan and R. C. G. Frem, *J. Solid State Chem.*, 2018, **260**, 67–72.
- 34 I. Imaz, M. Rubio-Martinez, J. An, I. Sole-Font, N. L. Rosi and D. MasPOCH, *Chem. Commun.*, 2011, **47**, 7287–7302.
- 35 A. C. Kathalikkattil, R. Babu, R. K. Roshan, H. Lee, H. Kim, J. Tharun, E. Suresh and D.-W. Park, *J. Mater. Chem. A*, 2015, **3**, 22636–22647.
- 36 G. S. Jeong, A. C. Kathalikkattil, R. Babu, Y. G. Chung and D. Won Park, *Chin. J. Catal.*, 2018, **39**, 63–70.
- 37 H. M. Perez-Cejuela, M. Mon, J. Ferrando-Soria, E. Pardo, D. Armentano, E. F. Simo-Alfonso and J. M. Herrero-Martinez, *Mikrochim. Acta*, 2020, **187**, 201.
- 38 S. A. Noorian, N. Hemmatinejad and J. A. R. Navarro, *J. Inorg. Biochem.*, 2019, **201**, 110818.
- 39 S. Wang, M. Wahiduzzaman, L. Davis, A. Tissot, W. Shepard, J. Marrot, C. Martineau-Corcoc, D. Hamdane, G. Maurin, S. Devautour-Vinot and C. Serre, *Nat. Commun.*, 2018, **9**, 4937.
- 40 L. Huang, L. Massa and J. Karle, *Quantum Biochem.*, 2010, **1**–60.
- 41 G. Chen, S. Huang, X. Kou, F. Zhu and G. Ouyang, *Angew. Chem., Int. Ed. Engl.*, 2020, **59**, 2–10.
- 42 A. Ghorbani-Choghamarani and Z. Taherinia, *Synth. Met.*, 2020, **263**, 116362.
- 43 H. Cai, Y.-L. Huang and D. Li, *Coord. Chem. Rev.*, 2019, **378**, 207–221.
- 44 L. Han, H. Zhang, D. Chen and F. Li, *Adv. Funct. Mater.*, 2018, **28**, 1800018.
- 45 C. Gu, H. Chen, Y. Wang, T. Zhang, H. Wang and G. Zhao, *Chemistry*, 2020, **26**, 3016–3021.
- 46 A. S. Ivanov and A. I. Boldyrev, *Org. Biomol. Chem.*, 2014, **12**, 6145–6150.
- 47 D. Feng, Z. Y. Gu, J. R. Li, H. L. Jiang, Z. Wei and H. C. Zhou, *Angew. Chem., Int. Ed. Engl.*, 2012, **51**, 10307–10310.
- 48 J. Wang, Y. Fan, Y. Tan, X. Zhao, Y. Zhang, C. Cheng and M. Yang, *ACS Appl. Mater. Interfaces*, 2018, **10**, 36615–36621.
- 49 Y. Zhang, F. Wang, C. Liu, Z. Wang, L. Kang, Y. Huang, K. Dong, J. Ren and X. Qu, *ACS Nano*, 2018, **12**, 651–661.
- 50 K. Kim, S. Lee, E. Jin, L. Palanikumar, J. H. Lee, J. C. Kim, J. S. Nam, B. Jana, T. H. Kwon, S. K. Kwak, W. Choe and J. H. Ryu, *ACS Appl. Mater. Interfaces*, 2019, **11**, 27512–27520.
- 51 J. Szejtli, *Chem. Rev.*, 1998, **98**, 1743–1753.
- 52 X. Hu, C. Wang, L. Wang, Z. Liu, L. Wu, G. Zhang, L. Yu, X. Ren, P. York, L. Sun, J. Zhang and H. Li, *Int. J. Pharm.*, 2019, **564**, 153–161.
- 53 I. Kritskiy, T. Volkova, T. Sapozhnikova, A. Mazur, P. Tolstoy and I. Terekhova, *Mater. Sci. Eng., C*, 2020, **111**, 110774.
- 54 N. Portolés-Gil, A. Lanza, N. Aliaga-Alcalde, J. A. Ayllón, M. Gemmi, E. Mugnaioli, A. M. López-Periago and C. Domingo, *ACS Sustainable Chem. Eng.*, 2018, **6**, 12309–12319.
- 55 Z. Li, Y. Peng, X. Pang and B. Tang, *ChemMedChem*, 2020, **15**, 13–16.
- 56 H. Zhang, Y. Shang, Y. H. Li, S. K. Sun and X. B. Yin, *ACS Appl. Mater. Interfaces*, 2019, **11**, 1886–1895.
- 57 X. Shen and B. Yan, *J. Mater. Chem. C*, 2015, **3**, 7038–7044.
- 58 G.-Y. Zhang, Y.-H. Zhuang, D. Shan, G.-F. Su, S. Cornier and X.-J. Zhang, *Anal. Chem.*, 2016, **88**, 11207–11212.
- 59 Y. Ma, H. Su, X. Kuang, X. Li, T. Zhang and B. Tang, *Anal. Chem.*, 2014, **86**, 11459–11463.
- 60 R. Xu, Y. Wang, X. Duan, K. Lu, D. Micheroni, A. Hu and W. Lin, *J. Am. Chem. Soc.*, 2016, **138**, 2158–2161.
- 61 H. Cai, W. Lu, C. Yang, M. Zhang, M. Li, C.-M. Che and D. Li, *Adv. Opt. Mater.*, 2019, **7**, 1801149.
- 62 Y.-Y. Liang, L.-J. Luo, Y. Li, B.-K. Ling, B.-W. Chen, X.-W. Wang and T.-G. Luan, *Eur. J. Inorg. Chem.*, 2019, 206–211.
- 63 Y. Liu, W. Hou, L. Xia, C. Cui, S. Wan, Y. Jiang, Y. Yang, Q. Wu, L. Qiu and W. Tan, *Chem. Sci.*, 2018, **9**, 7505–7509.
- 64 Z. Wang, Y. Fu, Z. Kang, X. Liu, N. Chen, Q. Wang, Y. Tu, L. Wang, S. Song, D. Ling, H. Song, X. Kong and C. Fan, *J. Am. Chem. Soc.*, 2017, **139**, 15784–15791.
- 65 J. Park, M. Xu, F. Li and H. C. Zhou, *J. Am. Chem. Soc.*, 2018, **140**, 5493–5499.
- 66 X. Gao, M. Zhai, W. Guan, J. Liu, Z. Liu and A. Damirin, *ACS Appl. Mater. Interfaces*, 2017, **9**, 3455–3462.
- 67 D. Chen, D. Yang, C. A. Dougherty, W. Lu, H. Wu, X. He, T. Cai, M. E. Van Dort, B. D. Ross and H. Hong, *ACS Nano*, 2017, **11**, 4315–4327.

